



HAL
open science

Comparison of four methods of surface roughness assessment of corneal stromal bed after lamellar cutting

Clotilde Jumelle, Alina Hamri, Gregory Egaud, Cyril Mauclair, Stéphanie Reynaud, Virginie Dumas, Sandrine Pereira, Thibaud Garcin, Philippe Gain, Gilles Thuret

► To cite this version:

Clotilde Jumelle, Alina Hamri, Gregory Egaud, Cyril Mauclair, Stéphanie Reynaud, et al.. Comparison of four methods of surface roughness assessment of corneal stromal bed after lamellar cutting. *Biomedical optics express*, 2017, 8 (11), pp.4974-4986. 10.1364/BOE.8.004974 . hal-01634361

HAL Id: hal-01634361

<https://hal.science/hal-01634361v1>

Submitted on 28 Oct 2024

HAL is a multi-disciplinary open access archive for the deposit and dissemination of scientific research documents, whether they are published or not. The documents may come from teaching and research institutions in France or abroad, or from public or private research centers.

L'archive ouverte pluridisciplinaire **HAL**, est destinée au dépôt et à la diffusion de documents scientifiques de niveau recherche, publiés ou non, émanant des établissements d'enseignement et de recherche français ou étrangers, des laboratoires publics ou privés.



Comparison of four methods of surface roughness assessment of corneal stromal bed after lamellar cutting

CLOTILDE JUELLE,¹ ALINA HAMRI,² GREGORY EGAUD,² CYRIL MAUCLAIR,^{2,3} STEPHANIE REYNAUD,³ VIRGINIE DUMAS,⁴ SANDRINE PEREIRA,⁵ THIBAUD GARCIN,^{1,6} PHILIPPE GAIN,^{1,6} AND GILLES THURET^{1,6,7,*}

¹Corneal Graft Biology, Engineering and Imaging Laboratory, BiiGC, EA2521, Federative Institute of Research in Sciences and Health Engineering, Faculty of Medicine, Jean Monnet University, 10 rue de la Marandière, 42055 Saint-Etienne Cédex 02, France

²GIE-Manutech-Ultrafast Surface Design, 20 rue Benoit Lauras, 42000 Saint-Etienne, France

³Hubert Curien Laboratory, UMR-CNRS 5516, Jean Monnet University, 18 rue Benoit Lauras, 42000 Saint-Etienne, France

⁴Ecole Nationale d'Ingénieurs de Saint-Etienne (ENISE), Laboratoire de Tribologie et Dynamique des Systèmes, UMR 5513 CNRS, 58 rue Jean Parot, 42023 Saint-Etienne, France

⁵Eye Bank, French Blood Center, 25 boulevard Pasteur, 42023 Saint-Etienne, France

⁶Ophthalmology Department, University Hospital, avenue Albert Raimond, 42055 Saint-Etienne Cédex 02, France

⁷Institut Universitaire de France, 1 rue Descartes, 75231 Paris, France

*gilles.thuret@univ-st-etienne.fr

Abstract: Corneal lamellar cutting with a blade or femtosecond laser (FSL) is commonly used during refractive surgery and corneal grafts. Surface roughness of the cutting plane influences postoperative visual acuity but is difficult to assess reliably. For the first time, we compared chromatic confocal microscopy (CCM) with scanning electron microscopy, atomic force microscopy (AFM) and focus-variation microscopy (FVM) to characterize surfaces of variable roughness after FSL cutting. The small area allowed by AFM hinders conclusive roughness analysis, especially with irregular cuts. FVM does not always differentiate between smooth and rough surfaces. Finally, CCM allows analysis of large surfaces and differentiates between surface states.

©2017 Optical Society of America

OCIS codes: (170.0170) Medical optics and biotechnology; (170.4470) Ophthalmology; (170.4580) Optical diagnostics for medicine; (000.1430) Biology and medicine; (120.0120) Instrumentation, measurement, and metrology; (120.6660) Surface measurements, roughness; (180.6900) Three-dimensional microscopy.

References and links

1. K. Stonecipher, T. S. Ignacio, and M. Stonecipher, "Advances in refractive surgery: microkeratome and femtosecond laser flap creation in relation to safety, efficacy, predictability, and biomechanical stability," *Curr. Opin. Ophthalmol.* **17**(4), 368–372 (2006).
2. C. A. Swinger and J. I. Barraquer, "Keratophakia and keratomileusis--clinical results," *Ophthalmology* **88**(8), 709–715 (1981).
3. A. Bernard, Z. He, F. Forest, A. S. Gauthier, M. Peoch, J. M. Dumollard, S. Acquart, R. Montard, B. Delbosc, P. Gain, and G. Thuret, "Femtosecond laser cutting of multiple thin corneal stromal lamellae for endothelial bioengineering," *Cornea* **34**(2), 218–224 (2015).
4. Z. He, F. Forest, A. Bernard, A. S. Gauthier, R. Montard, M. Peoc'h, C. Jumelle, E. Courrier, C. Perrache, P. Gain, and G. Thuret, "Cutting and Decellularization of Multiple Corneal Stromal Lamellae for the Bioengineering of Endothelial Grafts," *Invest. Ophthalmol. Vis. Sci.* **57**(15), 6639–6651 (2016).
5. P. Gain, R. Jullienne, Z. He, M. Aldossary, S. Acquart, F. Cognasse, and G. Thuret, "Global Survey of Corneal Transplantation and Eye Banking," *JAMA Ophthalmol.* **134**(2), 167–173 (2016).
6. K. Kamiya, H. Asato, K. Shimizu, H. Kobashi, and A. Igarashi, "Effect of Intraocular Forward Scattering and Corneal Higher-Order Aberrations on Visual Acuity after Descemet's Stripping Automated Endothelial Keratoplasty," *PLoS One* **10**(6), e0131110 (2015).

7. O. Muftuoglu, P. Prasher, R. W. Bowman, J. P. McCulley, and V. V. Mootha, "Corneal higher-order aberrations after Descemet's stripping automated endothelial keratoplasty," *Ophthalmology* **117**(5), 878–884 (2010).
8. M. Lombardo, M. P. De Santo, G. Lombardo, D. Schiano Lomoriello, G. Desiderio, P. Ducoli, R. Barberi, and S. Serrao, "Surface quality of femtosecond dissected posterior human corneal stroma investigated with atomic force microscopy," *Cornea* **31**(12), 1369–1375 (2012).
9. S. Serrao, L. Buratto, G. Lombardo, M. P. De Santo, P. Ducoli, and M. Lombardo, "Optimal parameters to improve the interface quality of the flap bed in femtosecond laser-assisted laser in situ keratomileusis," *J. Cataract Refract. Surg.* **38**(8), 1453–1459 (2012).
10. V. V. Mootha, E. Heck, S. M. Verity, W. M. Petroll, N. Lakshman, O. Muftuoglu, R. W. Bowman, J. P. McCulley, and H. D. Cavanagh, "Comparative study of descemet stripping automated endothelial keratoplasty donor preparation by Moria CBm microkeratome, horizon microkeratome, and Intralase FS60," *Cornea* **30**(3), 320–324 (2011).
11. M. M. Dickman, M. P. van Maris, F. W. van Marion, Y. Schuchard, P. Steijger-Vermaat, F. J. van den Biggelaar, T. T. Berendschot, and R. M. Nuijts, "Surface metrology and 3-dimensional confocal profiling of femtosecond laser and mechanically dissected ultrathin endothelial lamellae," *Invest. Ophthalmol. Vis. Sci.* **55**(8), 5183–5190 (2014).
12. M. A. Sarayba, T. S. Ignacio, P. S. Binder, and D. B. Tran, "Comparative study of stromal bed quality by using mechanical, IntraLase femtosecond laser 15- and 30-kHz microkeratomes," *Cornea* **26**(4), 446–451 (2007).
13. Z. Varga, C. Bergin, S. Roy, M. Nicolas, P. Tschuor, and F. Majo, "Scanning Electronic Microscopy Evaluation of the Roughness of the Stromal Bed After Deep Corneal Cut with the LDV Femtosecond Laser (Z6) (Ziemer) and the ONE Microkeratome (Moria)," *Curr. Eye Res.* **41**(10), 1302–1309 (2016).
14. Y. J. Jones, K. M. Goins, J. E. Sutphin, R. Mullins, and J. M. Skeie, "Comparison of the femtosecond laser (IntraLase) versus manual microkeratome (Moria ALTK) in dissection of the donor in endothelial keratoplasty: initial study in eye bank eyes," *Cornea* **27**(1), 88–93 (2008).
15. A. K. Riau, Y. C. Liu, N. C. Lwin, H. P. Ang, N. Y. Tan, G. H. Yam, D. T. Tan, and J. S. Mehta, "Comparative study of nJ- and μ J-energy level femtosecond lasers: evaluation of flap adhesion strength, stromal bed quality, and tissue responses," *Invest. Ophthalmol. Vis. Sci.* **55**(5), 3186–3194 (2014).
16. M. Fuest, S. Salla, P. Walter, N. Plange, D. Kuerten, A. Flammersfeld, and M. Hermel, "Comparison of Gebauer SLc and Moria CBm Carriazo-Barraquer ALK Microkeratomes for Descemet's Stripping Automated Endothelial Keratoplasty Preparation," *Curr. Eye Res.* **41**(3), 343–349 (2016).
17. M. Fuest, S. Salla, M. Hermel, W. J. Plum, S. Rütten, N. Plange, D. Kuerten, A. C. Schnitzler, and P. Walter, "Gebauer SLc Original and Moria One-Use Plus automated microkeratomes for ultrathin Descemet's stripping automated endothelial keratoplasty preparation," *Acta Ophthalmol.* **94**(8), e731–e737 (2016).
18. N. M. Ziebarth, J. Dias, V. Hürmeriç, M. A. Shousha, C. B. Yau, V. T. Moy, W. W. Culbertson, and S. H. Yoo, "Quality of corneal lamellar cuts quantified using atomic force microscopy," *J. Cataract Refract. Surg.* **39**(1), 110–117 (2013).
19. W. Kaplonek, K. Nadolny, and G. M. Królczyk, "The Use of Focus-Variation Microscopy for the Assessment of Active Surfaces of a New Generation of Coated Abrasive Tools," *Meas. Sci. Rev.* **16**(2), 42–53 (2016).
20. D. Tomida, T. Yamaguchi, A. Ogawa, Y. Hirayama, S. Shimazaki-Den, Y. Satake, and J. Shimazaki, "Effects of corneal irregular astigmatism on visual acuity after conventional and femtosecond laser-assisted Descemet's stripping automated endothelial keratoplasty," *Jpn. J. Ophthalmol.* **59**(4), 216–222 (2015).

1. Introduction

The cornea is the transparent lens-shaped tissue that forms the anterior part of the eye and provides two-thirds of its refractive power. It consists of approximately 300 collagen lamellae, arranged and interwoven in multiple directions for stiffness and optical properties. Corneal surgery involves removing, adding or replacing corneal tissue either to modify corneal shape during refractive surgery (one of the most common procedures being laser in situ keratomileusis (LASIK)) or to restore its transparency with the various corneal graft, or keratoplasty, techniques. The blade of a microkeratome (F) and more recently the light of a femtosecond laser (FSL) are commonly used during corneal surgery, chiefly to cut the superficial corneal flap during LASIK [1] or to cut lamellar grafts from donor corneas [2]. Lamellar cutting of multiple slices in one donor cornea is also being studied as a possibility to provide sufficient corneo-compatible carriers necessary to develop bioengineered endothelial grafts [3, 4], that could help reducing the huge scarcity for donor cornea worldwide [5]. The main risk of these intracorneal cuts parallel to the surface is of surface irregularities at the interface of cutting planes, which can result in optical aberrations causing a permanent drop in visual acuity [6, 7]. It is thus crucial to obtain the smoothest possible cutting plane. However, it is hard to determine which is the better technique, despite the number of comparative studies published in the past 10 years. Some show a relatively similar roughness of corneal

cuts for MKT and FSL [8, 9], while others favor MKT [10, 11] or FSL [12, 13]. This is due to at least three factors: 1/ the authors' use of various devices and cutting parameters, which are also continually being improved; 2/ the variability of the response of corneal tissue, of which the collagen structure organization and stiffness vary with depth and maybe also with age. The superficial flaps created by LASIK (80-120 μm under the corneal surface) are cut from collagen stiffer than that in the posterior cornea, which is cut for certain corneal grafts (500 μm under the surface); 3/ the lack of standardization between roughness-assessment techniques.

The most common method is a subjective roughness score applied to scanning electronic microscopy (SEM) [10, 14–17]. The next most common is the objective measure provided by atomic force microscopy (AFM) [8, 9, 11, 18]. However, different techniques produced different surface roughness values (all expressed in root mean square (RMS), see below), ranging from 0.09 to 1 μm for MKT (with AFM [8, 18]) and from 0.1 (with AFM [8]), to 2 μm (with a profilometer [11]) for FSL. Another important parameter is corneal hydration rate during observation (normally 78% (w/w) *in vivo*). Stable hydration should ideally be maintained as dehydration during examination could modify apparent roughness, especially if data acquisition is long. A controlled environment and/or high-speed acquisition could thus make roughness assessment more reliable.

In the present study, using human donor corneas cut in standardized conditions with a FSL, we compared four methods of assessing the surface quality of stromal cuts: SEM, AFM, chromatic confocal microscopy (CCM) and focus-variation microscopy (FVM) (Table 1).

Table 1. Main characteristics of the four microscopy methods used to measure surface roughness.

Technique	Lateral resolution (nm)	Vertical resolution (nm)	Acquisition time for a $10 \times 10 \mu\text{m}^2$ area
Scanning electron microscopy	1-10	?	A few seconds
Atomic force microscopy	10	<1	20 minutes
Confocal chromatic microscopy	900	8	1 minute
Focus-variation microscopy	800 to 2000	20 to 100	A few seconds

2. Methods

2.1 Corneal lamellae cutting

Human corneas unsuitable for transplantation for serological reasons and procured by the Auvergne-Loire and Besançon French eye banks (French blood centers) were used after informed consent of the relatives, as authorized by French bioethics laws. All procedures conformed to the tenets of the Declaration of Helsinki for biomedical research involving human subjects. Corneas were procured by *in situ* excision with 16 to 18 mm diameter trephination, according to the procedure recommended in France for corneas intended for transplantation. They were immediately immersed in 100 mL of storage medium (CorneaMax, Eurobio, Les Ulis, France) at 31°C in a dry incubator, in accordance with the preservation procedure of most European eye banks. The protocol used to prepare corneal lamellae was the same as that used in eye banks: 24 hours before cutting, corneas were deswelled in hyperosmotic solution (CorneaJet, Eurobio) to restore transparency and normal thickness.

Using an FSL, thin lamellae were cut from the posterior stroma, mimicking the cut of an endothelial keratoplasty. This type of keratoplasty corresponds to the selective replacement of only the posterior part of the cornea. It is used in frequent corneal diseases where only the endothelial cells are deficient. By convention, we chose to observe the surface state of the stromal side of the thin lamellae. During cutting, the cornea was mounted in a disposable anterior artificial chamber (Moria, Antony, France), pressurized at 40 mmHg in CorneaMax. To make a cutting plane approximately 200 μm above the Descemet membrane, an optical

coherence tomography system (SS-1000 CASIA, Tomey, Aichi-ken, Japan) was used prior to cutting, to map corneal thickness in order to choose the depth of FSL focus. The FSL cuts were made with a research FSL bench (Satsuma, Amplitude Systèmes, Pessac, France). This FSL generated 150 fs pulses at a 1030 nm central wavelength and a 250 kHz repetition rate. The FSL beam was displaced on a 10 mm XY surface using a scan head (IntelliSCAN III 14, SCANLAB, Puchheim, Germany) and then focused with a custom objective (Special Optics, Denville, NJ) allowing a spot diameter of 5.5 μm with a focal distance of 30 mm. A microscope glass slide, held by a homemade support adaptable on the anterior artificial chamber, was used to flatten the corneal surface as in other studies [3, 4]. The settings of our experimental FSL were similar to those of ophthalmological FSLs used in refractive surgery (such as the Abbott Intralase 150, the Alcon Wavelight FS200, and the Zeiss VisuMax) and were therefore likely to provide cutting planes with characteristics able to be extrapolated from what can be obtained with commercial laser.

After FSL cutting, corneas were trephined using an 8 mm diameter punch trephine (Katena, Denville, NJ) to isolate the 200 μm thick lamellae, which were immediately fixed in 0.1 M cacodylate-buffered 2% glutaraldehyde pH 7.4 at 4°C for at least 24 hours before observation and measurement.

To compare the four methods of roughness assessment (SEM, AFM, CCM and FVM) in standardized conditions, we first assessed the effect of sample dehydration and metallization on surface appearance with SEM, and on roughness measurement with CCM. CCM was chosen because it offers a useful compromise between high resolution in Z and acceptable acquisition speed. The purpose of these first two experiments was to study whether or not samples could be dehydrated and metallized (i.e. stabilized) without artefactually modifying their surface state. (Fig. 1).

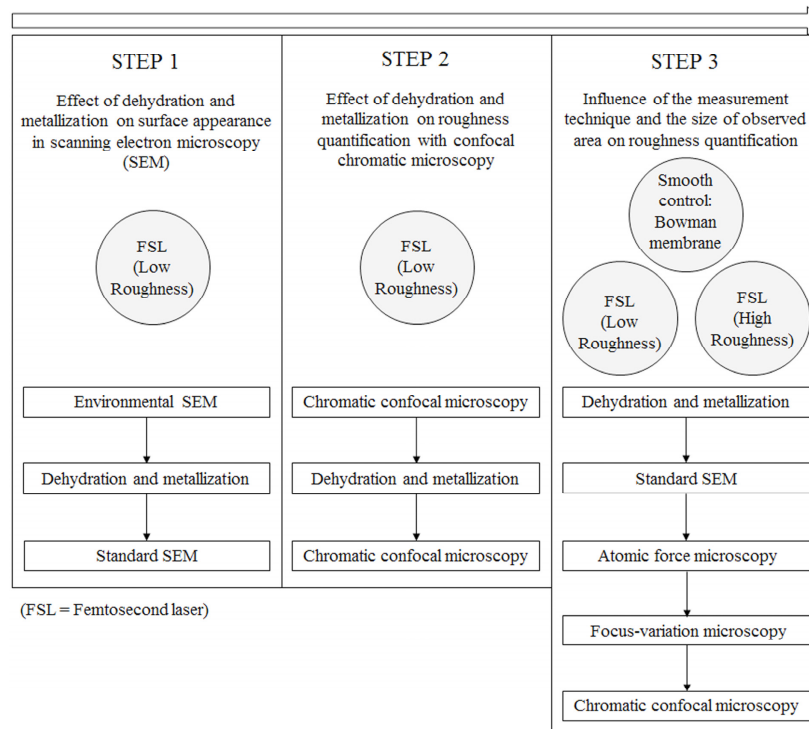


Fig. 1. Flow chart of experiments. Steps 1 and 2 were designed to study the influence on roughness measurement of stabilizing the samples by dehydration and metallization. In step 3, the three quantitative microscopy methods were compared.

2.2 Scanning electron microscopy

The Environmental SEM (eSEM) was used first because it theoretically allowed observation using more physiologic conditions i.e. not fully dehydrated and not metallized. Stromal lamellae were rinsed three times in 0.1 M cacodylate solution and then placed with the surface of interest (i.e. cutting plane) facing up on an aluminum stub. Observation was conducted with an eSEM (Quanta FEG 250, FEI, Hillsboro, OR) at a working distance of 9-10 mm and an accelerating voltage of 10 kV. The microenvironment in the chamber required to avoid dehydration of the lamella was maintained by a pressure of 5.4 Torr and a temperature of 6°C. Magnifications ranged from x40 to x50000 and secondary-electron images were acquired at a resolution of 1024 x 943 pixels.

After eSEM, lamellae were returned to the fixative solution for at least 24 hours at 4°C. The second SEM technology used was standard SEM (sSEM), which, unlike eSEM, required dehydration and metallization. Briefly, stromal lamellae were air-dried directly on a polished aluminum mount covered with double-coated carbon tape, with the surface of interest facing up. The lamellae being extremely thin (<200 µm), they were fully dry after 10 minutes. They were then coated with gold-palladium in a mini sputter coater (Polaron SC 7620, Quorum Technologies, Laughton, UK). Lamellae were then observed with an sSEM (S-3000N, Hitachi, Tokyo, Japan) at a working distance of 6-7 mm, an accelerating voltage of 5kV, and a vacuum between 10^{-4} and 10^{-5} Pascal. Magnifications ranged from x1 to x100000 and secondary-electron images were acquired at a resolution of 640 x 480 pixels.

2.3 Chromatic confocal microscopy

A chromatic confocal probe (CL1 MG 210, STIL, Aix-en-Provence, France) connected to a controller (CCS-Prima, STIL) was used to characterize the surface of stromal lamellae before and after dehydration and metallization. CCM was based on lateral scanning of the sample surface by incident white light imaged through a chromatic objective into a continuum of monochrome images along the Z axis. Only one wavelength of the continuum, depending on the height of the sample surface, was reflected into the optical system. After pinhole filtering, the reflected wavelength was analyzed by a spectrometer to determine the corresponding position of the sample surface. The sample surface was height mapped by measuring the reflected wavelength at each XY point. Lamellae were glued with adhesive paste (UHU, Baden, Germany) on a polished aluminum mount with surface of interest facing up. To reduce the risk of dehydration during observation, lamellae were hydrated with balanced salt solution (BSS, Alcon, Rueil-Malmaison, France) and excess water was removed with a surgical microsponge. Image acquisition took about 15 minutes at room temperature for a 300 x 300 µm² surface. After this first characterization, lamellae were returned to the fixative solution for 24 hours at 4°C, and were then dehydrated and metallized per the same protocol as for the sSEM. A second characterization was then performed on the dehydrated and metallized sample. For each characterization by CCM, three non-overlapping surfaces of 300 x 300 µm² were characterized for three lamellae cut by FSL from three corneas.

The first two experiments demonstrated the absence of artifact after dehydration and metallization (see results). Several stromal lamellae were thus cut by FSL from different donor corneas, then dehydrated, metallized and flat mounted as described above. They were observed with sSEM and separated into two groups: low and high surface roughness. It is known that the same FSL cutting parameters can give different surface states according to parameters including transparency, donor age, depth of cut into cornea, and other unknown individual donor parameters. One lamella in each group was used to compare the three microscopes (AFM, FVM, CCM). The denuded Bowman's membrane (BM) served as a control, given its naturally extremely smooth surface. The BM is the outer corneal membrane situated directly beneath the epithelium. It was obtained by gently scraping the epithelium

from a cornea and FSL cutting 200 μm beneath the surface. The control lamellae were dehydrated and metallized as described above, and flat mounted with the BM facing up.

2.4 Atomic force microscopy

An AFM (Agilent 5500, Keysight Technologies, Santa Rosa, CA) equipped with a silicon microcantilever tip (ACT, Applied NanoStructures, Mountain View, CA) was used in a non-contact mode, also called acoustic AC mode, which is less sensitive but also less destructive than the contact mode typically used in the literature. The sample surface was scanned by a cantilever tip which oscillated owing to the vibrations of a piezoelectric crystal supporting the tip. The closer the cantilever tip was to the sample surface, the lower the resonance frequency of oscillation, due to the presence of Van der Waals forces at the sample surface. A feedback loop system adjusted the tip-sample distance, maintaining the resonance frequency around 300 kHz. The sample surface was height mapped by measuring the tip-sample distance at each XY point.

2.5 Focus-variation microscopy

Focus-variation microscopy was performed with an InfiniteFocus IF G4 (Alicona, Raaba/Graz, Austria). The Z depth of the sample surface was scanned by a white light beam through a microscope objective, magnification of which depended on the observed area and on the image resolution. An observed area of 1.62 x 1.62 mm^2 , 0.81 x 0.81 mm^2 and 0.32 x 0.32 mm^2 , a working distance of 1.62 mm, 0.81 mm and 0.32 mm, a lateral resolution of 800, 1000 and 2000 nm and a vertical resolution of 20, 50 and 100 nm and were obtained respectively with x10, x20 and x50 objectives. The white light beam was reflected into a photoelectric detector inside the optical system and, for each Z-plane, in-focus zones were detected by a processing signal unit to allow height mapping of the sample surface [19]. The manufacturer XYZ calibrated the microscope using certified gage blocks.

For the three lamellae (low/high roughness, smooth control), four non-overlapping surfaces of 10x10 μm^2 , 100x100 μm^2 , 300x300 μm^2 and 1000x1000 μm^2 were acquired from each lamella by FVM and CCM to assess the effect of surface area on roughness measurement. For AFM, only the 10x10 μm^2 size was acquired, acquisition time for larger areas being too long.

2.6 Image analysis of surface roughness

All images acquired by the three microscopes were analyzed with Mountains, a surface imaging and metrology software program (Digital Surf, Besancon, France), to calculate height-map roughness. Raw data measured by the three devices were imported into the software that accepted multiple format files. The use of the same methods of surface roughness calculation eliminated the bias linked to differences between the software programs of each instrument. Each height map was converted by the software into two roughness profile series, along the X and Y axes. Roughness was calculated to ISO 4287 (1997, Geometrical product specifications – Surface texture: profile method – Terms, definitions and surface texture parameters), as illustrated in Fig. 2. The roughness profile was defined as being derived from the primary profile by suppressing the long-wave component (high-pass) filter, with cut-off being λ_c . Parameters were designated R and evaluated within the evaluation length, which generally consists of five sampling lengths. The sampling length corresponds to the cut-off wavelength λ_c of the profile filter. As stated in ISO 16610 (2011 geometrical product specifications – Filtration – Part 21: Linear profile filters), a Gaussian filter was used on the roughness profiles with different λ_c values according to the observed area: $\lambda_c = 2.5 \mu\text{m}$ for 10 x 10 μm^2 , $\lambda_c = 25 \mu\text{m}$ for 100 x 100 μm^2 , and $\lambda_c = 80 \mu\text{m}$ for 300 x 300 μm^2 and 1000 x 1000 μm^2 . This filtering of the roughness profile series removed the macro-waviness liable to result from folds caused by non-optimal flat mounting, and thus kept only the actual surface roughness caused by the cutting technique. For each profile, a mean line

corresponding to the mean roughness of the profile was generated. The length of each profile was cut into five sampling lengths and for each section the root mean square roughness R_{RMS} , also called quadratic mean roughness, was calculated. This was determined by Eq. (1), where z is the height between the mean line and the profile, and n the number of heights of the section:

$$RMS = \sqrt{\frac{1}{n} \sum_{i=1}^n z_i^2} \quad (1)$$

The mean R_{RMS} of the five sections was then calculated to obtain the RMS of the total profile. The mean R_{RMS} of the total profile was calculated to obtain the R_{RMS} of the total profile series. The final R_{RMS} (expressed in nanometers) was calculated as the mean of the RMS of both profile series along the X or Y axis. For example, the RMS of a perfectly smooth surface would be 0 nm. Figure 2 presents the schematic calculation. For each lamella, three non-overlapping surfaces were acquired and analyzed, and the mean and standard deviation of the surface roughness were calculated.

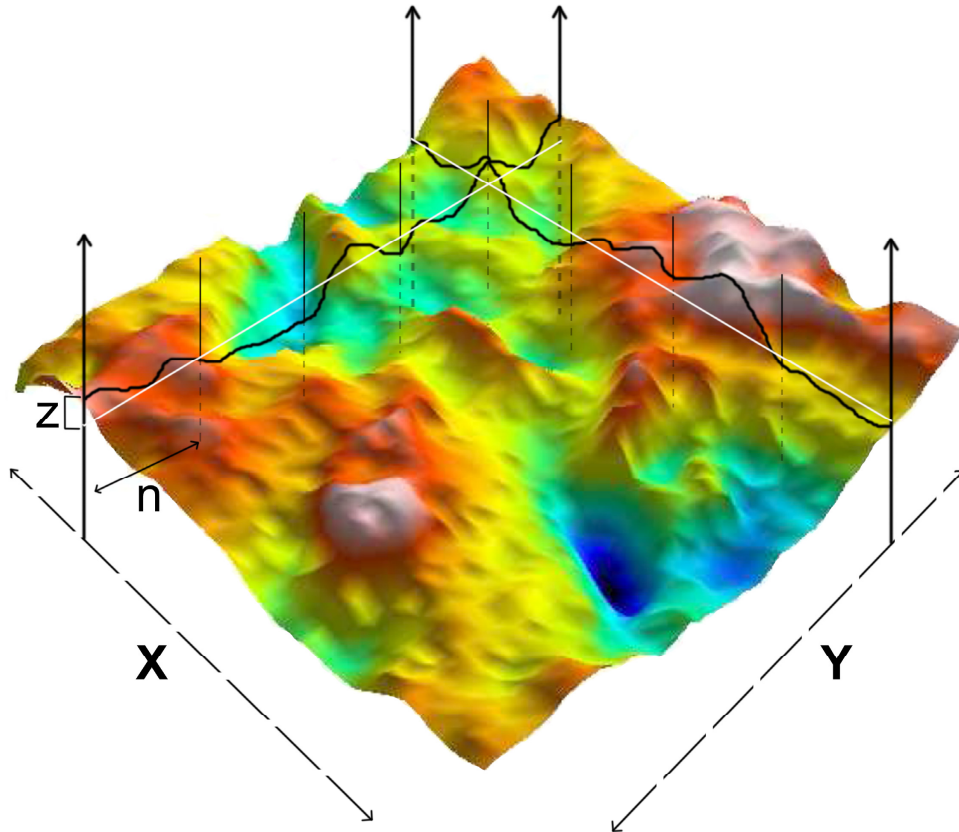


Fig. 2. Method of roughness calculation. Example of an X profile and a Y profile from a height map (black line). 1/ Mean straight lines (white lines) were generated for each X and Y profile. 2/ Each profile was separated into five sampling lengths. 3/ R_{RMS} was calculated for each segment, with the n being the number of Z-heights measured between the X (or Y) profile and its associated mean straight line. 4/ For each X or Y profile, the profile- R_{RMS} was calculated as the mean R_{RMS} of its five sampling lengths. 5/ X- R_{RMS} and Y- R_{RMS} were calculated as the mean of all profiles along the X or Y axis. 6/ Lastly, total- R_{RMS} was calculated as the mean of X-mean R_{RMS} and Y-mean R_{RMS} .

2.7 Statistical analysis

Data were described by their median (25-75th percentiles) and compared using non-parametric tests with post-hoc tests for pairwise comparisons. Statistical analysis was performed using SPSS 23.0 (SPSS, Chicago, IL) with $p < 0.05$ deemed significant. Individual results and their median are stated in all figures for greater clarity.

3. Results

3.1 Effect of dehydration and metallization on surface appearance by scanning electron microscopy

Surface appearance was generally similar with eSEM and sSEM (Fig. 3), but image contrast was lower with eSEM than with sSEM. This difference between the two microscopes was higher for FSL cut lamellae, which presented the smallest structures likely corresponding to melted-like photo-disrupted collagen fibers. Consequently, the subsequent observations were performed only with sSEM.

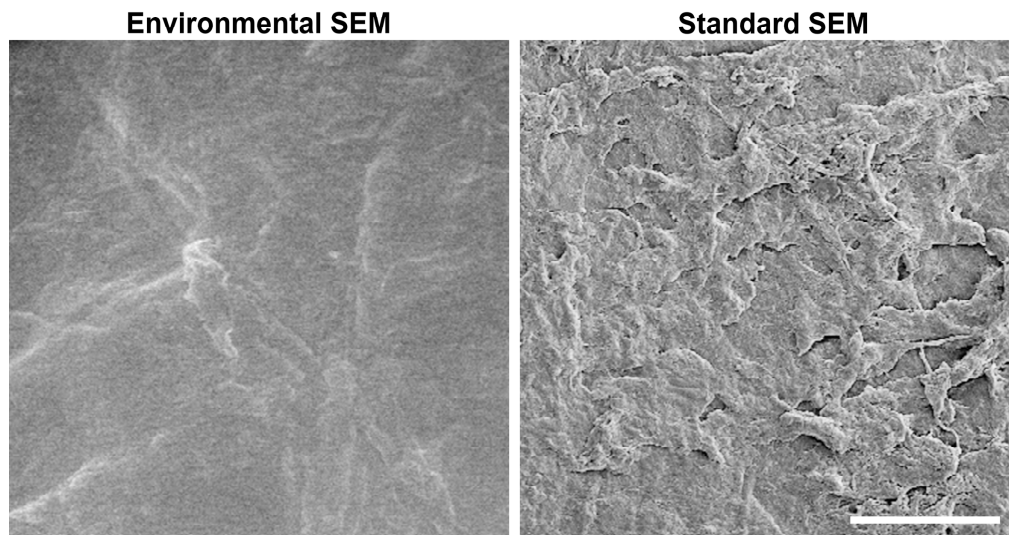


Fig. 3. Comparison of environmental and standard scanning electron microscopy using a surface state obtained after corneal cutting with a femtosecond laser. Both images are displayed with the same magnification. Scale bar = 100 μm .

3.2 Effect of dehydration and metallization on roughness measurement by chromatic confocal microscopy

For the three lamellae cut by FSL, surface roughness measured by CCM did not differ between measurements performed on hydrated lamellae and after dehydration and metallization, with an RMS of 330, 365 and 412 before treatment and of 359, 385, 397 after treatment (paired data, $P = 0.285$ Wilcoxon test). The subsequent experiments were thus performed with dehydrated, metallized tissues.

3.3 Influence of measurement technique on roughness measurement

The visual rendering and roughness values of lamellae surfaces differed greatly according to the microscope used, especially in the high-roughness group. The three techniques were compared only for the $10 \times 10 \mu\text{m}^2$ analysis area, i.e. the maximum reasonably measurable by AFM (it took 20 minutes to assess a $10 \times 10 \mu\text{m}^2$ with AFM). For this small area, AFM and CCM but not FVM provided significantly rising values for the three surface states (smooth, low/high roughness). For the smooth control, the three microscopes provided similar values.

For the low and high roughness surfaces, CCM provided significantly higher values than the two others (Fig. 4).

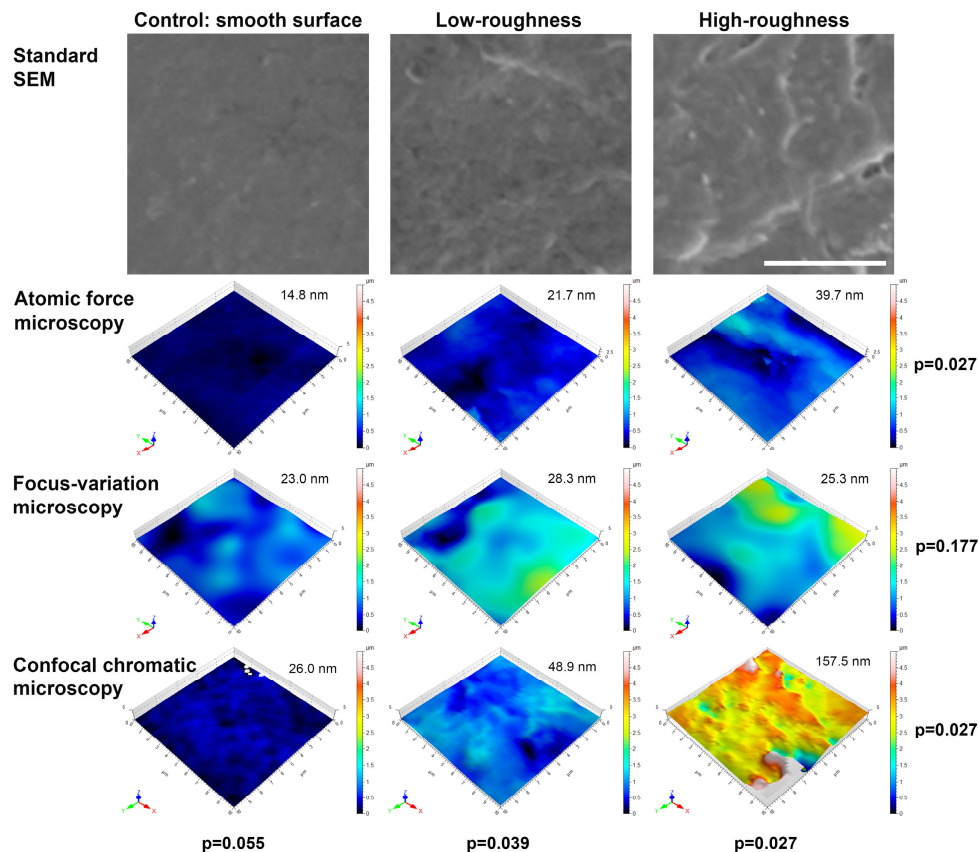


Fig. 4. Direct comparison of scanning electron microscopy and the three quantitative methods (atomic force microscopy, focus-variation microscopy, chromatic confocal microscopy). Lamellae with low and high roughness were compared with the naturally smooth surface of the Bowman membrane (BM, control). $10 \times 10 \mu\text{m}^2$ areas selected at random were compared. The surface of the same lamellae appeared different on the height-maps provided by the three microscopes, especially in the high-roughness group. Each height-map was presented with its roughness value expressed in nm. For the same sample, roughness values varied from 1 to 4 according to the measurement methods. Statistics: Kruskal-Wallis tests. P values were indicated for each row and each column. Scale bar = $5 \mu\text{m}$.

3.4 Influence of observed area on roughness measurement

FVM and CCM, unlike AFM, allowed roughness measurement on surfaces larger than $10 \times 10 \mu\text{m}^2$. Figure 5 shows the 3D maps of three areas ($100 \times 100 \mu\text{m}^2$, $300 \times 300 \mu\text{m}^2$ and $1000 \times 1000 \mu\text{m}^2$) for the same three corneal lamellar surface states previously observed (smooth, low/high roughness). Visual rendering and roughness values of the surface of the same lamellae differed according to the technique and to the area analyzed (Fig. 5). FVM values were significantly higher than CCM values ($P = 0.002$ Mann-Whitney test). FVM values increased with surface roughness for $100 \times 100 \mu\text{m}^2$ ($P = 0.027$) and $300 \times 300 \mu\text{m}^2$ ($P = 0.027$), but not for $1000 \times 1000 \mu\text{m}^2$ ($P = 0.193$). Conversely, CCM always differentiated between the three surface states, whatever the area analyzed ($P = 0.027$ for all), as for $10 \times 10 \mu\text{m}^2$ as stated above.

For both methods, roughness values significantly increased when the area analyzed increased (except for the smooth surface analyzed by CCM). This increase was observed for

the three surface states (Figs. 5 and 6). However, CCM values stayed in the same order of magnitude (maximum of $\times 2.3$), whereas FVM values ranged from 1 to 4.6 and the highest increase was observed for the smooth surface.

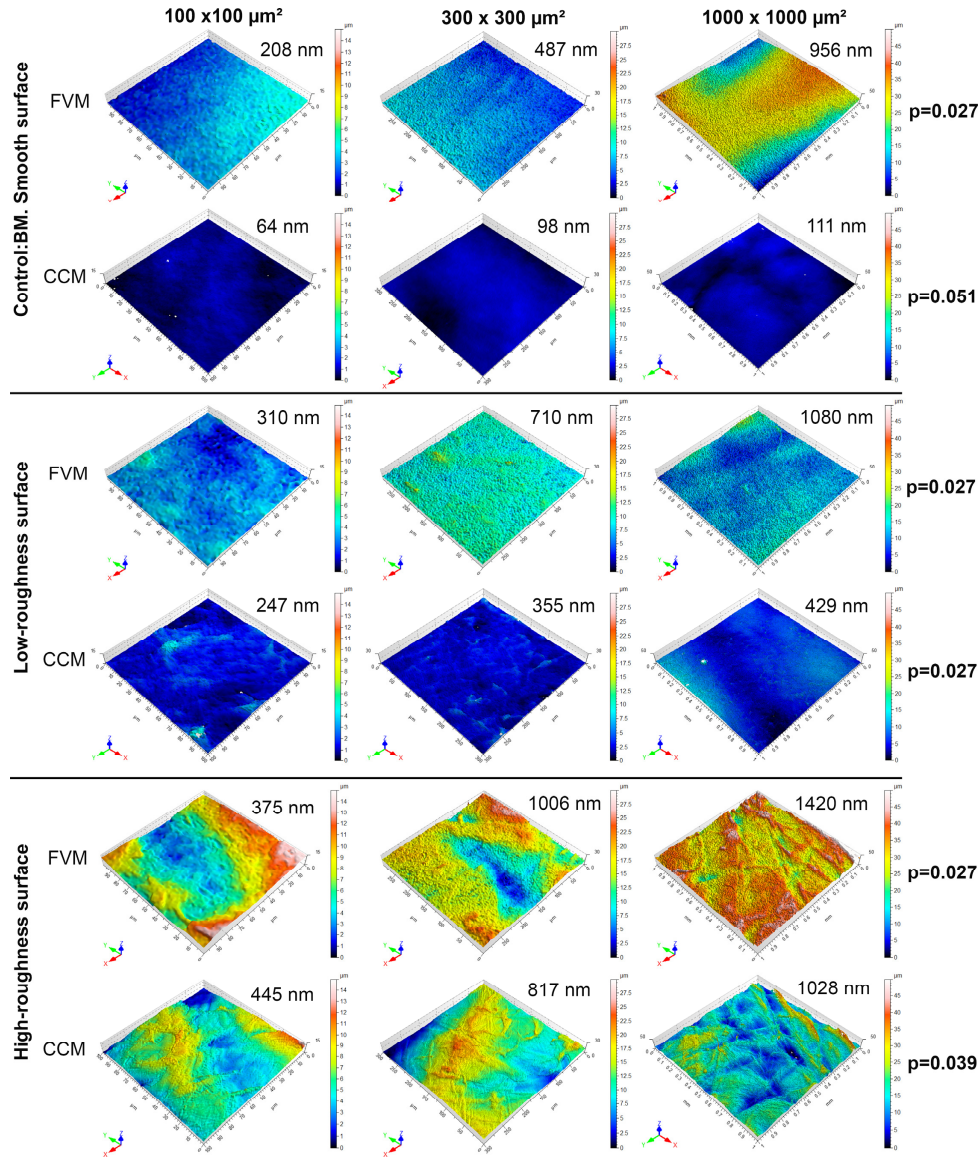


Fig. 5. Influence of area observed by focus-variation (FVM) and chromatic confocal microscopy (CCM) on roughness measurement. 3D maps of lamellae with smooth, low-roughness and high-roughness surfaces. For each lamella, areas of $100 \times 100 \mu\text{m}^2$, $300 \times 300 \mu\text{m}^2$ and $1000 \times 1000 \mu\text{m}^2$ were characterized by FVM and CCM. Each height-map is associated with its roughness value in nm.

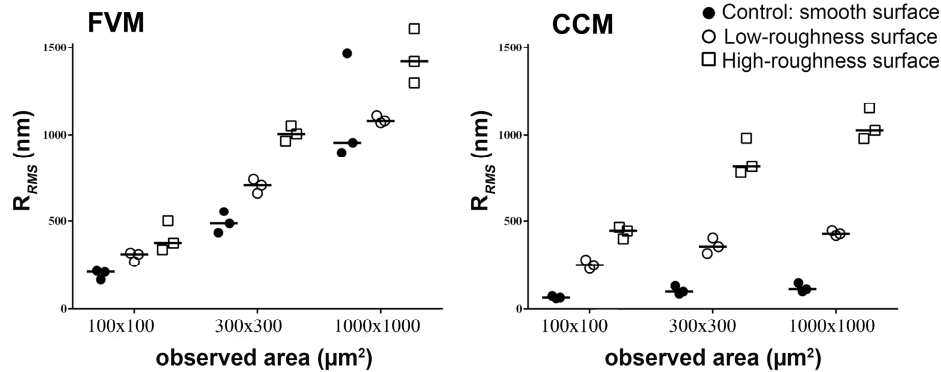


Fig. 6. Surface roughness mean and error of three corneal lamellar surfaces (smooth, low/high roughness) per surface area (100x100 μm^2 , 300x300 μm^2 , 1000x1000 μm^2) and characterization technique (focus-variation microscopy (FVM) or chromatic confocal microscopy (CCM)).

4. Discussion

The present study directly compared two qualitative techniques (eSEM, sSEM) and three quantitative techniques (AFM, FVM, CCM) for the assessment of surface roughness of cutting planes obtained after corneal surgical cutting. During lamellar corneal surgery, stromal surface irregularities due to low-quality cutting can lead to poor visual outcomes [20]. Smoother is generally better. However, there is no clear quantitative definition of a smooth stromal surface. This is why reliable surface assessment is a crucial step in validating a cutting technique or new cutting parameters for an existing technique. However, up to now, the various qualitative and quantitative techniques for surface roughness assessment described in the literature gave highly variable roughness values, making it difficult indirectly to compare surface states. The difficulty is further increased by the use of various measurement methods to assess various cutting methods.

For practical reasons, we chose to work with ex vivo human corneas cut with an FSL and not with live laboratory animals. The standardized samples that we obtained enabled us to compare the different measuring devices. In addition, they were representative of donor corneas cut for different purposes, such as endothelial transplantation or bioengineering. Note that the same measuring devices could be used to assess any other corneal surface, such as cuts done in live corneas during animal experiments.

Our protocol, which compares various techniques performed on the same corneal samples and uses a step-by-step process, controls selection bias caused by variation of roughness between tissues. However, it does not ensure that the three microscopes analyze exactly the same area, especially with small areas. This point argues for analysis of the largest possible areas and/or repetition of measurements on the same specimen, to take account of possible local roughness variations.

The aspect of the stromal surface was found to be similar with both SEM techniques, showing that the dehydration and metallization required for sSEM did not affect surface appearance. On the contrary, sSEM provided better contrast and thus better qualitative assessment. For this application, eSEM can thus not be recommended. We also showed with CCM that sample preparation did not cause roughness value bias. We strongly recommend dehydrated, metallized corneal samples, given their advantages over fresh specimens (storage, possibility of reexamination).

The three quantitative microscopes provide different roughness values and can thus not be used interchangeably. For this application, FVM was least reliable. Unlike AFM and CCM, it only distinguished roughness differences on 100x100 and 300x300 μm^2 areas. AFM and CCM differentiated on all sizes, but CCM gave a wider range of roughness values than AFM

(for a given area), suggesting CCM is more sensitive. In the present study, we deliberately chose three very different sample types. In real life, as more subtle differences between surface states must be measured, CCM seems a better candidate than AFM.

This study showed that roughness is highly dependent on the measurement technique (for which lateral and vertical resolution vary), and observed area. The lack of harmonization of techniques described for roughness measurement of corneal surface in the literature makes it almost impossible to compare surface quality between studies. It is thus crucial to consider roughness as a relative parameter that must be compared with a control. Above all, the BM, which is highly reproducible, can serve as a smooth control and a target to be achieved by optimizing the corneal cut process. The best way to characterize the roughness of any material (biological or not) is still by using several techniques, as in this study.

Our study has some limitations. Maintaining sample hydration during our CCM acquisition of hydrated tissue is subject to caution. On the one hand, the hydration rate may influence the qualitative and quantitative roughness assessments: excess water could form a layer at the sample surface and hide some of the reliefs, while dehydration could trigger collagen fiber retraction and artificially increase surface relief. On the other hand, it seems near impossible to ensure the same hydration rate among samples when roughness is measured, as the hydration rate of corneal lamellae depends on at least three parameters: their thickness, time spent outside the humidified chamber, and temperature. By demonstrating that dehydration and metallization have no significant influence on surface appearance or roughness values, we eliminated this difficulty and resolved not to assess corneal specimens in their physiologic environment. Finally, lamella metallization may have a negative impact, as bright surfaces are not recommended for FVM characterization. Our decision, which also considered the long acquisition time and the difficulty of maintaining hydration as discussed above, was pragmatic.

In the literature, AFM is the most common method for measuring roughness of corneal lamellar cutting. Although authors in the literature commonly use AFM in contact mode in humidified chambers, we preferred a non-contact mode on metallized samples to avoid the risk of surface damage by the AFM tip. Despite high resolution, the long acquisition time restricts observed area and thus the representativeness of the roughness value. Recently, Dickman et al. measured larger surfaces with a topography profiler comparable to FVM (both use the same optical principle) [11]. These technologies allow high-speed acquisition and thus characterization of larger surfaces versus AFM. Dickman et al. obtained a surface roughness of $2 \mu\text{m}$ for a surface of $255 \times 191 \mu\text{m}^2$. With our FVM, we obtained half the roughness for the high-roughness lamella (up to $1 \mu\text{m}$ for a surface of $300 \times 300 \mu\text{m}^2$). This difference highlights that surface roughness is a relative parameter, even when similar techniques are used.

All the aforementioned methods are only intended for experimental use of *in vitro* samples. Considering the present results, and the fact that the principle of CCM seems compatible with *in vivo* use, further work will be necessary to first assess the feasibility of roughness assessment immediately after corneal cutting in live animals.

5. Conclusion

Compared to FVM and AFM, CCM is a relatively new technology for roughness characterization, and to our knowledge has not yet been used on corneal tissue. It appears a reliable alternative combining sufficient resolution, large field of observation, and acceptable acquisition time. Chromatic confocal microscopy may thus be recommended for the objective comparison of corneal cutting methods.

Funding

Agence Nationale pour la Recherche: SupCo 2014 ANR-14-CE16-0008-01.

Disclosures

The authors have no proprietary or commercial interest in any materials discussed in this article.

Acknowledgements

We would like to thank Isabelle Anselme and Nora Mallouk-Forges from the Centre de microscopie électronique Stéphanois, and Anne Rivoire, Christelle Boule and Xavier Jaurand from the Centre Technologique des Microstructures (Claude Bernard University) for their assistance with scanning electron microscopy.